

Energy Storage Siting and Sizing in the WECC Area and the CAISO System

Ricardo Fernández-Blanco, Yury Dvorkin, Bolun Xu,
Yishen Wang, and Daniel S. Kirschen*

June 9, 2016

Abstract

Spatio-temporal arbitrage using energy storage systems reduces the cost of operating a power system. However, since the cost of deploying storage is significant, it is essential to determine the optimal locations and ratings of these systems. This paper proposes a stochastic storage siting and sizing method that determines the optimal locations and ratings. This is first done from a centralized perspective where the objective is to minimize the sum of the operating and investment costs. The method is then modified to combine this cost minimization with the perspective of an investor who wants to find the storage locations and ratings that will maximize its profits.

The effectiveness of the centralized method is demonstrated on a 240-bus, 448-line model of the WECC system. The combined perspective is analysed using a 4754-bus and 6377-transmission line model of the CAISO system.

The effect of adding constraints on the maximum number of locations where storage can be installed and on the size of energy storage systems is discussed. Sensitivity analyses are also performed to assess the impact of the investment cost and of the value attached to avoiding spillage of renewable energy. We also consider how a significant increase in the marginal costs of conventional generators and in the renewable generation capacity would affect these results.

*The authors are with the Department of Electrical Engineering, University of Washington, Seattle, WA, 98195 USA (e-mail: rfbc85@uw.edu; dvorkin@uw.edu; ywang11@uw.edu; xubolun@gmail.com; and kirschen@uw.edu).

Contents

1	Introduction	3
2	Storage siting and sizing from a centralized perspective	4
2.1	Problem formulation	4
2.2	Case study	4
2.3	Optimal siting decisions	4
2.4	Optimal sizing decisions	6
2.5	Cost savings and renewable energy spillage	8
2.6	Profitability of energy storage	8
2.7	Effect of the maximum rating of energy storage systems	9
2.8	Effect of the cost of thermal generation	10
2.9	Effect of the proportion of production from renewable sources	12
2.10	Simultaneous effect of the cost of thermal generation and proportion of production from renewable sources	15
3	Combining cost minimization and profitability of storage	17
3.1	Problem formulation	17
3.2	Case study	17
3.3	Base case	17
3.4	Balancing cost and profit	18
3.5	Effect of the number of storage locations	19
4	Conclusions	22
	Appendices	23
A	Nomenclature	23
B	Mathematical formulation of the cost minimization problem	25
C	Mathematical formulation of the multi-objective problem	28
D	Handling of fixed generation	30

1 Introduction

The integration of grid-scale energy storage (ES) in power systems is motivated by their proven ability to support the large-scale deployment of renewable generation [1]. The techno-economic benefits provided by ES have been demonstrated for various applications on different planning and operational timescales and for several storage technologies [1, 2]. Castillo *et al.* [2] categorize grid-scale applications of ES in power-related services, such as regulation and voltage control, and energy-related services, such as spatio-temporal energy arbitrage, load following, and congestion management. Given these applications, the U.S. Department of Energy projects that the ES business could grow to be a “\$19 billion industry by 2017” [3]. There is thus a need for decision-making tools able to optimize the locations and capacities of ES for realistically large transmission grids. This problem is known in the technical literature as ES optimal siting and sizing.

We discuss the ES optimal siting and sizing problem from two perspectives. First, we consider the perspective of a System Operator (SO) who has the authority to choose ES locations and sizes in a way that minimizes the sum of the operational and investment costs. Then we combine the perspective of the SO with the perspective of a profit-seeking ES owner in a multi-objective optimization framework [4].

In the first problem, the SO is interested in choosing locations and ratings for storage that would reduce the operating cost through spatio-temporal arbitrage, i.e. charging and discharging storage at different times and locations. As customarily assumed [5], the proposed investment model is static, i.e. investment decisions are optimized for operation during a future target year. System operation during this target year is modeled using representative days. The SO then aims to minimize the expected operating and the daily pro-rated investment costs over the set of representative days of the target year. This problem accounts for the following constraints:

1. commitment and dispatch decisions of conventional generators;
2. dispatch decisions on renewable generators;
3. dispatch decisions on energy storage;
4. transmission constraints represented by a dc power flow model.

The problem is solved using mixed-integer linear programming (MILP) solvers. The effects of ES integration are quantified on a reduced model of the Western Electricity Coordinating Council (WECC) system with 240 buses and 448 transmission lines.

To combine the perspective of the SO and of the storage owner, we re-formulate the problem as a multi-objective optimization. [4]. In this problem, we combine the system costs of the SO and the profits collected by the ES owner into a single objective function subject to the technical constraints defined in the first problem. The profits collected by ES are weighted with a parameter ranging from 0 to 1 to study how the profit motive affects siting and sizing decisions. This combined perspective is analysed using a 4754-bus and 6377-transmission line model of the CAISO system based on the WECC 2024 planning model.

2 Storage siting and sizing from a centralized perspective

2.1 Problem formulation

From a centralized perspective, the siting and sizing of energy storage should be such that it minimizes the sum of the operating cost and of the investment cost, subject to constraints on the operation of the system and on the size and location of the investments in energy storage. Appendix B shows how this problem can be formulated mathematically as a Mixed Integer Linear Programming (MILP) problem. Since one of the reasons for deploying energy storage is to assist in the integration of renewable energy sources such as wind and solar, and since these resources have a stochastic output, this optimization relies on a stochastic formulation.

2.2 Case study

This optimization was applied to the simplified model of the WECC system described in [6], whose network consists of 240 buses, 448 transmission lines, 157 aggregated conventional generators (71 thermal units, 27 hydropower plants) and a substantial renewable generation portfolio (3 biomass, 6 geothermal, 11 generic renewable, 7 solar, and 32 wind farms). Five representative days were used to represent the variety of load and renewable conditions that should be expected. These days and the weight that each of them should have in the objective function were selected using the recursive hierarchical clustering algorithm described in [7].

An energy-to-power ratio of 6 hours was selected for prospective ES investments [8, 9]. ES charging and discharging efficiencies are assumed to be 0.9. Two capital cost scenarios were considered: In the Low Investment Cost (LIC) scenario, the cost of energy storage system is assumed to be \$20/kWh and \$500/kW, while in the High Investment Cost (HIC) scenario, it is assumed to be \$100/kWh and \$1500/kW. These investment costs are prorated on a daily basis assuming an ES lifetime is 10 years and an annual discount rate is 5%, as explained in [8]. We assume that energy storage can be installed at any bus in the system.

To account for future increases in the operating cost of fossil-fuel generators (e.g. due to a carbon tax), the marginal cost of the thermal units was multiplied by a factor of 2, unless otherwise specified. The production from renewable sources was increased by 40% to simulate California's renewable energy goal for the year 2030 [10], unless otherwise stated.

All simulations were carried out on an Intel Xenon 2.55 GHz processor with 32 GB of RAM using the Hyak supercomputer system at the University of Washington, [11] running CPLEX [12] under GAMS 23.7 [13]. The stopping criterion for all simulations was reaching a 1% optimality gap.

2.3 Optimal siting decisions

Table 1 summarizes the optimal ES siting decisions as a function of several parameters:

1. the capital cost of deploying energy storage (LIC and HIC scenarios);
2. the value attached to spillage of renewable energy sources V_{oRS} (According to [14], we assume that the value of renewable spillage ranges from \$0/MWh to \$80/MWh.)
3. the maximum number of locations where energy storage can be installed (1, 5, 10, and 15 locations). ES systems located at each bus have a maximum energy rating of $\bar{S} = 25$ MWh.

These results show that bus 155 is clearly the preferred location for the deployment of energy storage because storage is located there when only deployment is allowed at only one location and when deployment is allowed at 5, 10 or 15 locations, regardless of the value of V_{oRS} and the

capital cost scenario. This bus is connected to a transmission line that is prone to congestion. Buses 90, 150, and 239, are selected as potential ES locations for all values of $VoRS$. All these buses are at the end of congested transmission lines.

For the HIC scenario, the optimization determines that installing storage at all 10 or 15 buses is not economically justifiable, except for $VoRS = 80\$/MWh$.

The Venn diagram of Fig. 1 shows the similarity between the siting decisions for $N^{ES} = 10$ and different values of $VoRS$.

TABLE 1. STORAGE SITING DECISIONS. IMPACT OF THE INVESTMENT COST, $VoRS$, AND N^{ES} .

Investment cost	VoRS	Maximum number of storage locations						
		1	5	10	15			
LIC	0	155	90	88	142	33	89	142
			150	89	150	80	90	160
			155	90	155	82	91	228
			228	91	228	87	140	239
			239	140	239	88	141	240
	40	155	27	22	30	88	148	198
			28	23	90	89	149	225
			90	26	150	90	150	226
			150	27	155	140	154	227
			155	28	239	142	155	239
	80	155	90	31	150	29	148	224
			150	33	155	30	149	225
		155	49	226	33	150	226	
		226	90	227	89	155	227	
		227	148	239	90	198	239	
HIC	0	155	88	90		26	88	141
			89	155		27	89	142
			90			28	90	155
			150			29	91	239
			155			30	140	
	40	155	89	80	150	33	90	150
			90	83	155	82	91	155
			150	88	239	83	140	227
			155	89		88	141	239
			239	90		89	142	
	80	155	90	82	155	88	142	224
			150	83	198	89	148	225
		155	89	226	90	150	226	
		226	90	227	91	155	227	
		227	150	239	140	198	239	

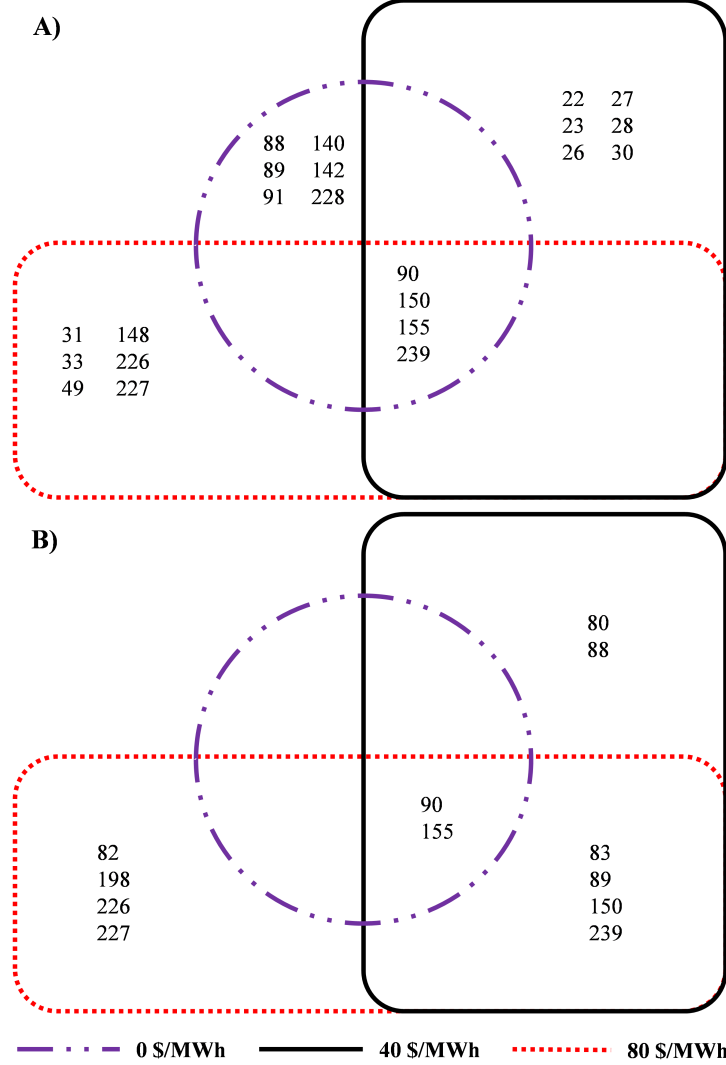


Fig. 1. Venn diagram for the storage siting decisions corresponding to $N^{ES} = 10$ buses: A) Low investment cost scenario, and B) high investment cost scenario.

2.4 Optimal sizing decisions

Figures 2 and 3 show the ES sizing decisions corresponding to the siting decisions shown in Table 1.

As one would expect, the amount of energy storage installed under the HIC scenario is usually smaller than under the LIC scenario.

For the LIC, the optimization deploys at each bus the maximum energy rating allowed at each bus (\bar{S}).

For the highest $VoRS$, the total installed power capacity increases linearly with the number of storage locations N^{ES} . For lower $VoRS$, this total installed power capacity tends to saturate as the number of locations increases.

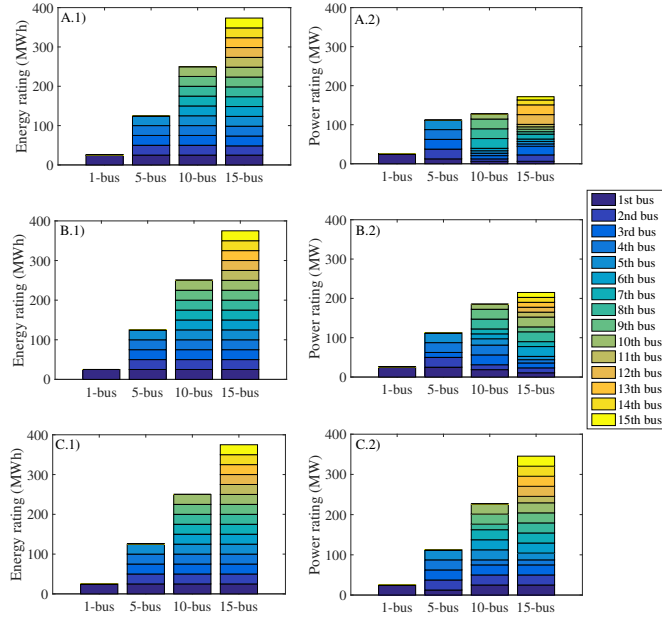


Fig. 2. Energy and power ratings for the low investment cost scenario: A.1)–A.2) $VoRS = 0$ \$/MWh, B.1)–B.2) $VoRS = 40$ \$/MWh, and C.1)–C.2) $VoRS = 80$ \$/MWh.

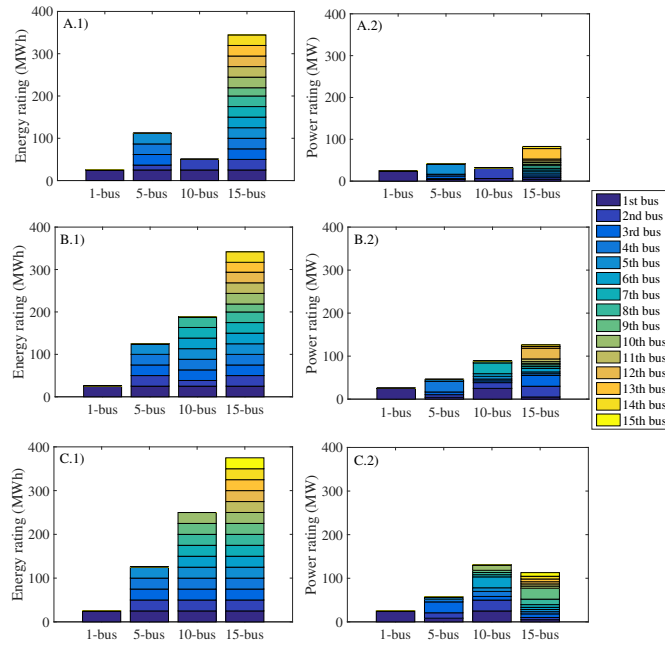


Fig. 3. Energy and power ratings for the high investment cost scenario: A.1)–A.2) $VoRS = 0$ \$/MWh, B.1)–B.2) $VoRS = 40$ \$/MWh, and C.1)–C.2) $VoRS = 80$ \$/MWh.

2.5 Cost savings and renewable energy spillage

For a given amount of investment, performing spatio-temporal reduces the system operating cost (i.e. the fuel cost). Fig. 4 shows the savings achieved for both capital cost scenarios, for the various number of storage locations and $VoRS$. These savings are below 1% for this case study. Furthermore, they decrease as $VoRS$ increases as the emphasis shifts to avoiding spilling energy produced by renewable sources.

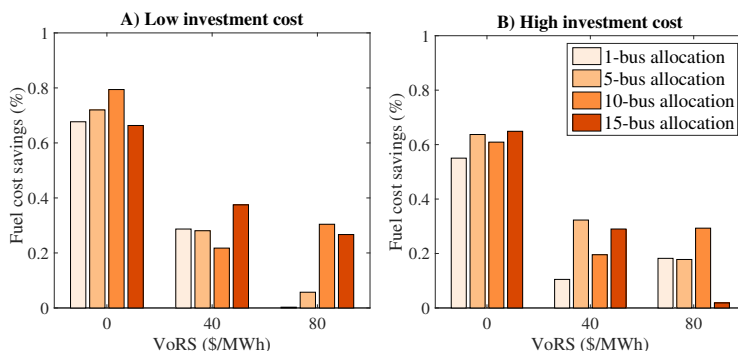


Fig. 4. Fuel cost savings for: A) Low investment cost scenario, and B) high investment cost scenario.

Fig. 5 shows how renewable energy spillage is reduced for these various conditions. Note that this reduction is a by-product of the optimization process and is not explicitly minimized. This explain it increases in some cases.

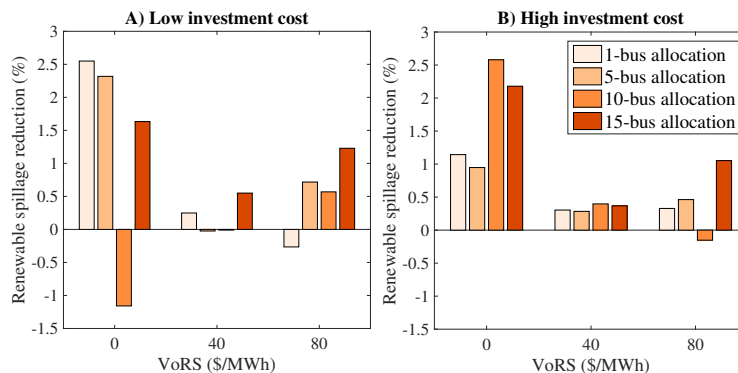


Fig. 5. Reduction of renewable spillage for: A) Low investment cost scenario, and B) high investment cost scenario.

2.6 Profitability of energy storage

While this model focuses on determining the location and size of storage that would minimize the total *cost*, it is useful to consider how profitable storage would be under these conditions. Fig. 6 shows the operating profit collected by the energy storage systems if they bought and sold the energy they charge and discharge at the marginal price for the bus where they are located. The operational profit increases with the number of ES locations and $VoRS$.

However, the operating profit is only one side of profitability. Taking into account the investment cost, Fig. 7 shows the rate of return ratio of energy storage, i.e. its ability to recover the investment cost. These results show that ES is profitable only for a small number of ES locations

in the LIC scenario. In general, this rate of return ratio increases with $VoRS$. Policy decisions that discourage spillage of energy produced from renewable energy sources could therefore significantly improve the profitability of investments in energy storage. This rate of return ratio decreases with the number of ES locations regardless of $VoRS$ or the capital cost scenario. This suggests that a coordinated strategy for investments in energy storage may be needed to ensure the economic viability of these investments.

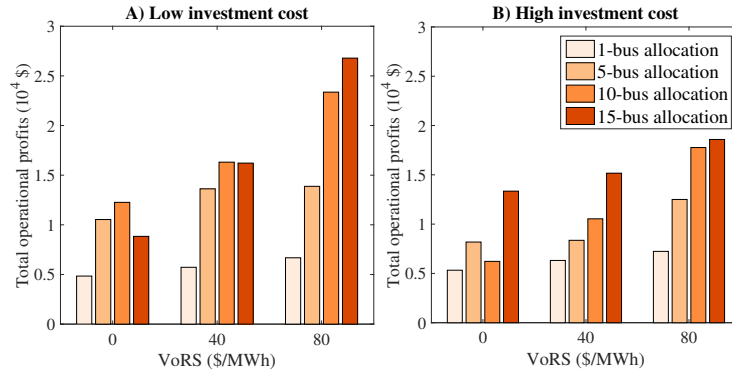


Fig. 6. Operating profit of energy storage for: A) Low investment cost scenario, and B) high investment cost scenario.

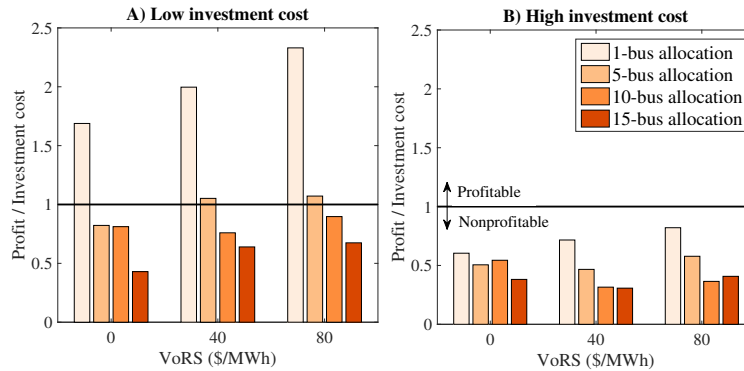


Fig. 7. Rate of return ratio of energy storage for: A) Low investment cost scenario, and B) high investment cost scenario.

2.7 Effect of the maximum rating of energy storage systems

Since energy storage systems are quite large, it is reasonable to assume that the amount of storage that can be installed at each bus is limited. In the previous sections, this amount was limited to $\bar{S} = 25$ MWh per bus. In this section, we gradually increase \bar{S} up to 100 MWh per bus for the LIC scenario, with $VoRS = 0$ \$/MWh, and $N^{ES} = 10$.

Figures 8 and 9 show how the optimal siting and sizing decisions change as we increase \bar{S} . These results show that the siting decisions are robust with respect to the maximum energy rating of energy storage at each bus. Specifically, buses 90, 150, 155, and 239 remain the best locations for all cases. In terms of the sizing decisions, Fig. 9 shows that the energy ratings are limited by \bar{S} and that the power ratings increase with this parameter.

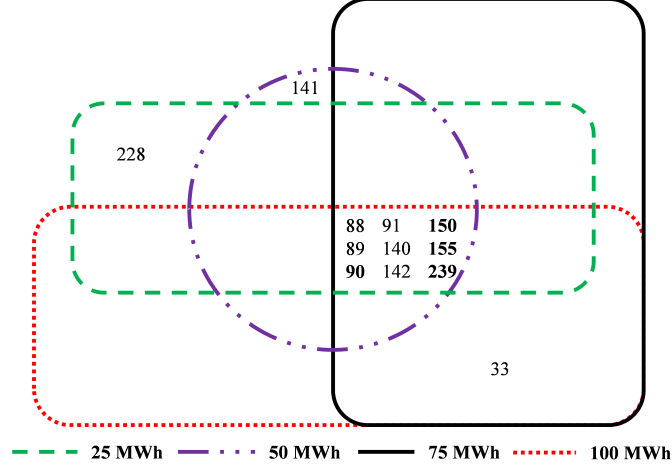


Fig. 8. Venn diagram showing how optimal storage siting decisions change as a function of the maximum energy storage rating per bus \bar{S} . The numbers in bold are the common storage locations regardless the $VoRS$ for the low investment cost.

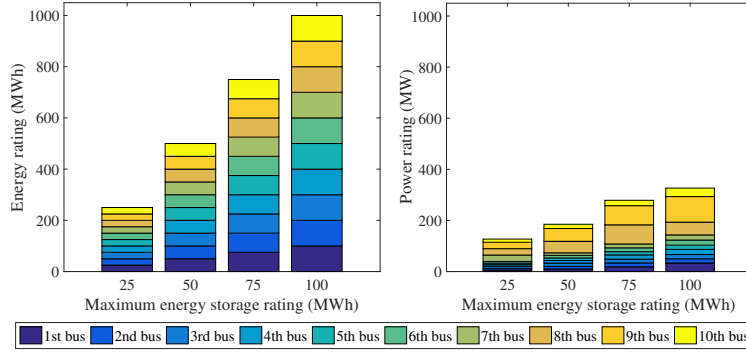


Fig. 9. Effect of the maximum energy storage rating per bus \bar{S} on the energy and power ratings.

Figure 10 shows the effect of \bar{S} . The cost savings (A) and the operating profits (B) increase with \bar{S} , while the amount of renewable energy spilled displays a non-monotonic behavior (C). Although the operating profit increases, the rate of return ratio decreases due to the higher investment cost (D).

2.8 Effect of the cost of thermal generation

An increase in the cost of thermal generation, coupled with an increase in the amount of energy produced from renewable energy sources, is likely to increase arbitrage opportunities. We analyze this effect by progressively increasing the marginal cost of conventional thermal generators. We consider the LIC scenario, with $VoRS = 0$ \$/MWh, $N^{ES} = 10$, and $\bar{S} = 100$ MWh because this is the case providing the largest cost savings. In this case, there is a 49.6% of installed renewable generation capacity including hydropower with respect to the overall installed capacity.

Figure 11 is a Venn diagram which shows that the siting decisions remain quite robust as the marginal cost is multiplied by a factor ranging from 1 to 5. In particular, buses 90, 150, 155, and 239 are selected as optimal locations irrespective of the value of this marginal cost.

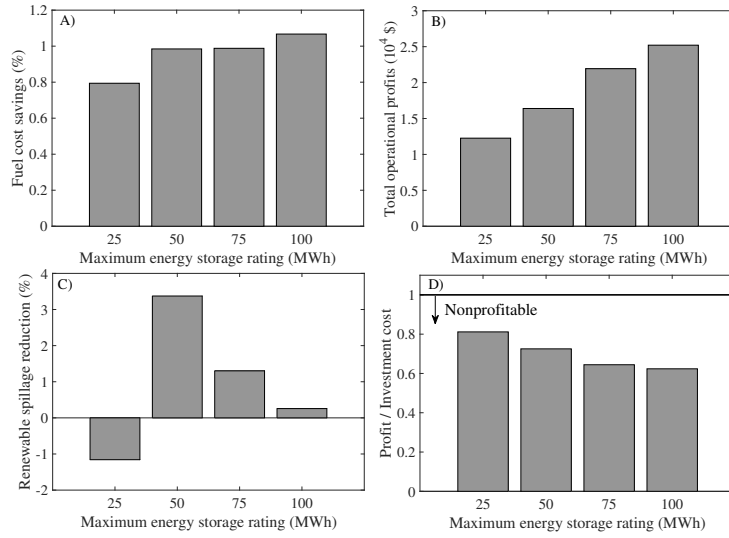


Fig. 10. Effect of the maximum energy rating \bar{S} on A) fuel cost savings, B) operating profits, C) reduction in renewable energy spillage, and D) ES rate of return ratio.

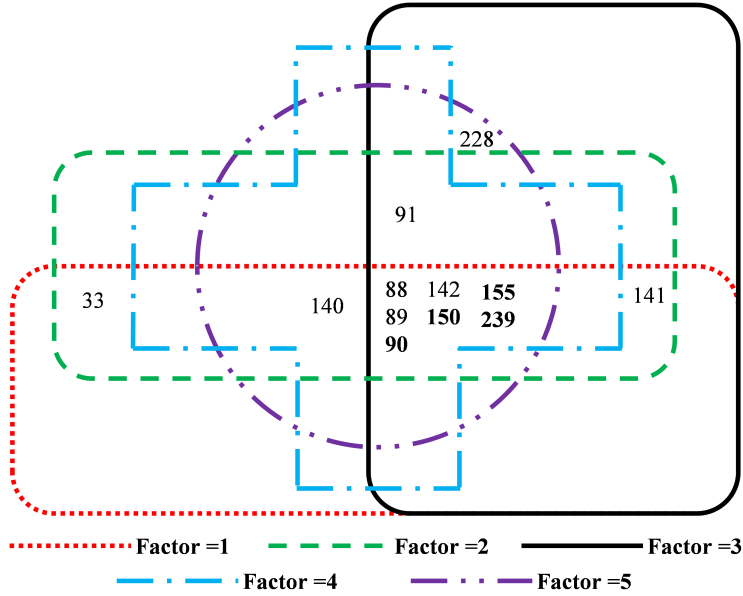


Fig. 11. Venn diagram showing the effect of the marginal costs of conventional generators on the optimal storage siting decisions. The numbers in bold are the common storage locations regardless the V_{oRS} and the maximum energy storage rating per bus S for the low investment cost.

Fig. 12 shows that the optimal total power rating of BESS tends to saturate as the marginal costs of thermal generation increases.

Figure 13 shows how this marginal cost increase would affect the cost savings, the operational profit, the amount of renewable energy spillage reduction and the rate of return of energy storage.

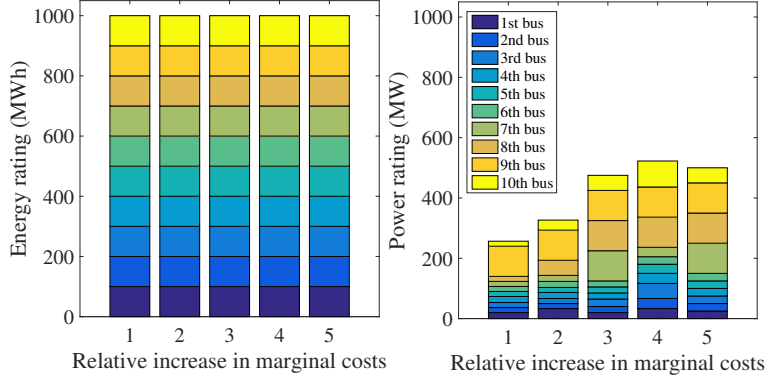


Fig. 12. Effect of the marginal costs of thermal generators on the energy and power ratings of energy storage.

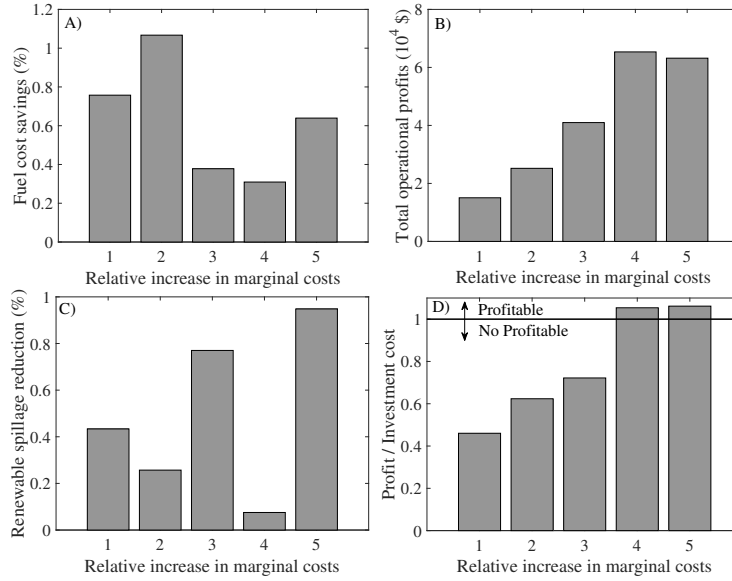


Fig. 13. Effect of the marginal costs of conventional thermal generators on A) Fuel cost savings, B) operational profits, C) reduction of renewable spillage, and D) ES rate of return ratio.

2.9 Effect of the proportion of production from renewable sources

To study the effect of stringent renewable energy goals similar to those imposed by the state of California by 2030 or Hawaii for the years 2030 and 2040 [10], the original renewable production is multiplied by a factor ranging from 1 to 1.8. We assume that the locations of this renewable production remain unchanged. The other fixed parameters are the same as in the previous section.

The Venn diagram of Fig. 20 shows that once again the ES siting decisions remain robust against changes in the penetration of renewable production. Buses 90, 150, 155, and 239 are still selected regardless of the renewable scenario. On the other hand, the optimal power ratings (Fig. 15) do not increase with the renewable penetration. This effect has an impact on the fuel cost savings and operational profits given in Fig. 16, which shows that the maximum cost savings are not attained for the maximum renewable penetration. However, an increased renewable penetration improves the operating profits and the rate of return ratio of energy storage and reduces the

amount of renewable energy spilled.

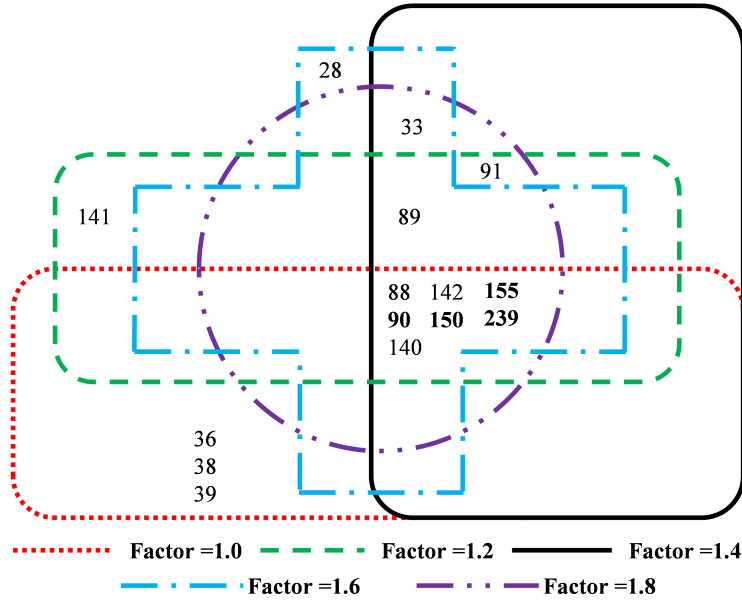


Fig. 14. Venn diagram showing the effect of renewable production on optimal storage siting decisions. The numbers in bold are the common storage locations regardless the $VoRS$, the maximum energy storage rating per bus \bar{S} , and the marginal costs of thermal generators for the low investment cost.

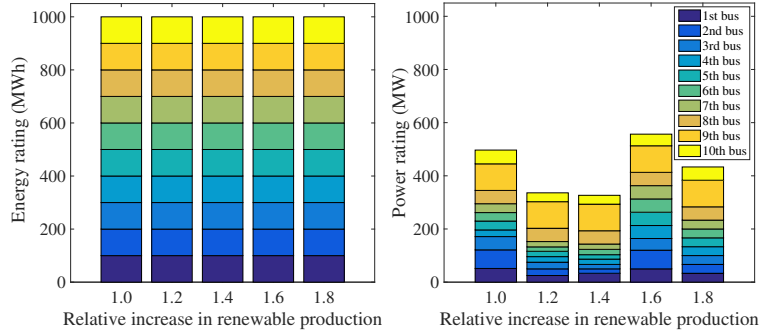


Fig. 15. Effect of renewable production on the optimal energy and power ratings.

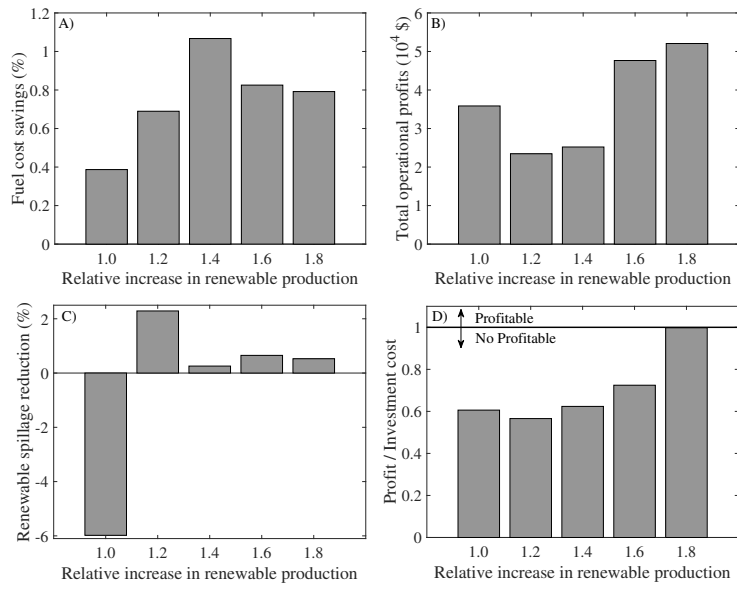


Fig. 16. Effect of renewable production on A) fuel cost savings, B) operational profits, C) reduction of renewable spillage, and D) ES rate of return ratio.

2.10 Simultaneous effect of the cost of thermal generation and proportion of production from renewable sources

Assuming the case providing the largest cost savings, i.e. LIC scenario, with $VoRS = 0$ \$/MWh, $N^{ES} = 10$, and $\bar{S} = 100$ MWh, we analyze the effect of simultaneous increases in the cost of thermal generation and in the amount of energy produced from renewable energy sources. This scenario is a realistic anticipation of what might happen in coming years: as the amount of renewable energy production increases, the cost of conventional generation is likely to increase to compensate for the fact that these generators will produce less but will still have to cover their fixed costs. Five cases are simulated by increasing the original cost of thermal generation and the original renewable production by the following factors: 1 and 1 (case a), 2 and 1.2 (case b), 3 and 1.4 (case c), 4 and 1.6 (case d), and 5 and 1.8 (case e).

Fig. 17 shows the Venn diagram for this simultaneous effect and we can see again the robustness against changes in both the cost of thermal generation and the amount of renewable production. Buses 90, 150, 155, and 239 (in bold) are selected as locations for energy storage regardless of the case. In Fig. 18, we can observe that the optimal power ratings of energy storage increases with each of these cases.

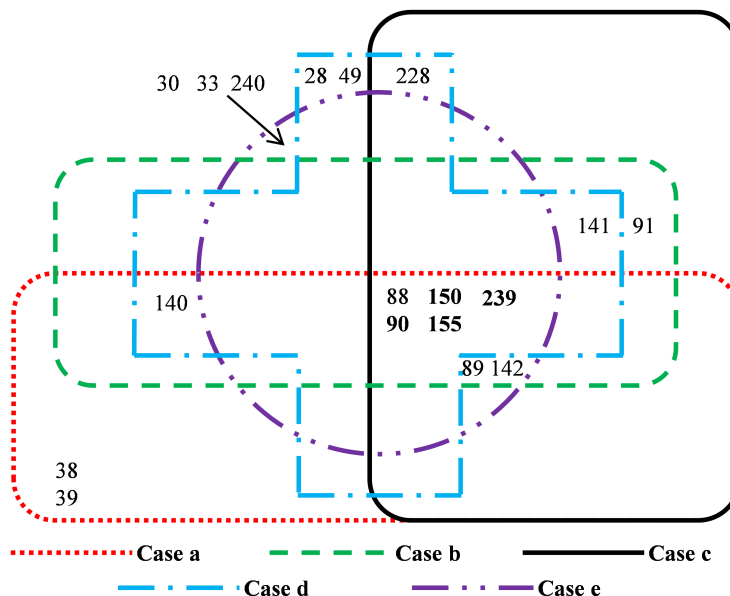


Fig. 17. Venn diagram showing the effect on the optimal storage siting decisions of a simultaneous increase in the cost of thermal generation and in renewable production. The numbers in bold are the common storage locations regardless of the $VoRS$, of the maximum energy storage rating per bus \bar{S} , and the individual effects of the cost of thermal generation and renewable production.

Fig. 19 shows that the minimum fuel cost savings are not attained with the maximum renewable penetration when this is accompanied by an increase in the cost of thermal generation. However, we can observe a monotone increase in the operating profits of storage. We can also see the same pattern in the rate of return ratio of investments in energy storage. Finally, as observed in other analyses, the amount of renewable energy spilled depends on the case considered.

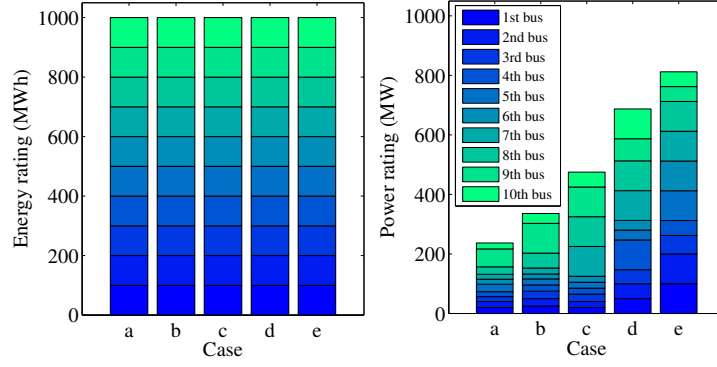


Fig. 18. Effect of renewable production on the optimal energy and power ratings.

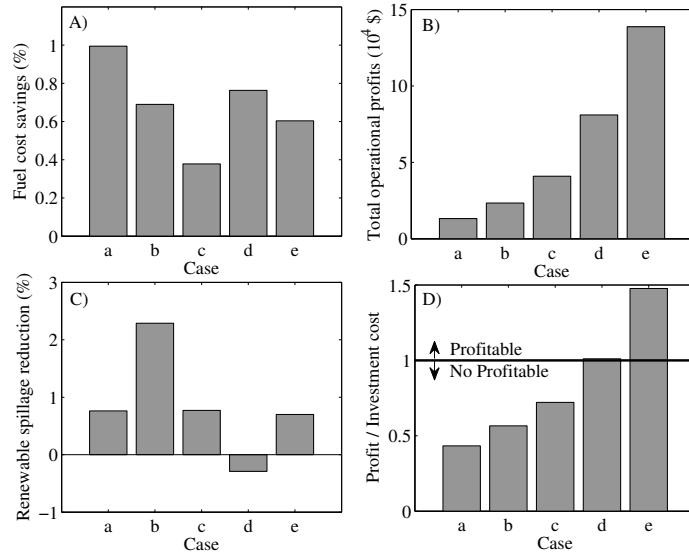


Fig. 19. Effect of renewable production on A) fuel cost savings, B) operating profit of energy storage, C) reduction in renewable energy spillage, and D) ES rate of return ratio.

3 Combining cost minimization and profitability of storage

3.1 Problem formulation

In a competitive electricity market environment, investments in energy storage systems will be made by for-profit entities. While the availability of these storage devices should lower the cost of operating the system, this is not the same as maximizing the operating profit collected by energy storage systems. The objectives of the system operator and of the storage owners are thus not aligned. We formulate a multi-objective optimization problem, which combines the cost minimization with the profit maximization. By adjusting the weight given to each part of the objective function, we can study the interactions between the goals of the system operator and the storage owner.

Appendix C provides a detailed mathematical formulation of this multi-objective optimization problem and a description of a two-stage algorithm that makes possible its application to large-scale systems.

3.2 Case study

This multi-objective optimization approach was applied to a model of the CAISO system based on the WECC 2024 planning model. Table 2 summarizes the characteristics of this system. As in the previous problem, investments decisions are based on 5 representative days and their associated weights determined using the recursive hierarchical clustering algorithm described in [7]. An energy-to-power ratio of 6 hours was selected for prospective ES investments [8,9]. Energy storage charging and discharging efficiencies are assumed to be 0.9.

TABLE 2. CHARACTERISTICS OF THE CAISO SYSTEM MODEL.

Controllable generators	316
Buses	4,754
Transmission Lines	6,377
Wind generators	117
Solar generators	414
Uncontrollable resources or fixed generation	1,182

In order to reduce the computational burden and to focus on the multi-objective problem, we perform siting and sizing decisions for the Sacramento Municipal District area which has 245 buses. We assume that spilling renewable energy has a value of 50 \$/MWh, and that the maximum number of locations where storage can be installed is 10. We consider only the lower investment cost scenario (500 \$/kWh and 20 \$/kW) and we limit the maximum energy storage rating at each bus to 50 MWh. The locational marginal prices are assumed to be equal to those resulting from the system cost minimization problem without ES. Generation considered as "fixed" in the WECC model occasionally needs to be reduced to ensure feasibility. Appendix D discusses the policies used to determine fixed generation spillage.

3.3 Base case

We establish a base case by solving the cost minimization problem for the system without energy storage. We first perform this optimization for each representative day separately and one stochastic optimization. We then perform a stochastic optimization where each representative day is weighted by the number of days in the cluster it represents. These results give us a basis to

assess the benefits of integrating energy storage in the system. Table 3 shows the total generation cost, the total renewable spillage including solar and wind assets, and the total fixed generation spillage for each representative day and for the stochastic optimization.

TABLE 3. COSTS FOR THE BASE CASE WITHOUT ENERGY STORAGE

	Generation cost (\$)	Renewable spillage (MW)	Fixed spillage (MW)
Day 1	4328530.9	25521.8	28435.1
Day 2	10764202.5	15.1	59081.0
Day 3	13336594.2	7855.6	64688.0
Day 4	3823475.6	39079.2	28120.7
Day 5	11005584.4	1218.8	55147.3
Stochastic	9030299.8	12096.4	47727.7

3.4 Balancing cost and profit

The formulation of the multi-objective optimization problem involves a parameter β which weighs the importance given to the profit collected by the energy storage systems. If the value of this parameter is zero, this profit is not taken into account in the optimization. We perform simulations for 4 values of the parameter β (0.001, 0.01, 0.1 and 1), thus giving an increasing weight to the maximization of the profit over the minimization of the cost. Table 4 gives the ten best locations for siting storage for each value of β . Four locations (buses 4337, 4375, 4376, 4523) are selected for all these values of β . On the other hand, two buses (2374 and 4361) are selected only for $\beta = 0.001$ which almost neglects the profit part of the objective function. These are buses that would be of interest to the system operator but not to independent investors.

Figure 20 shows the optimal energy and power ratings for all energy storage locations given in Table 4. The energy rating is limited by the artificially imposed 500 MWh bound. The power rating increases slightly as the profit maximization gains more importance in the objective function.

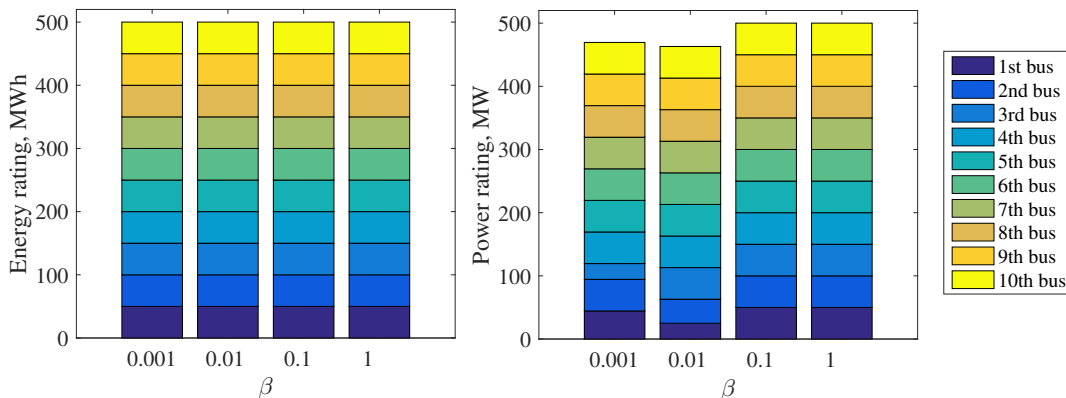


Fig. 20. Optimal energy and power ratings for weights of the profit motive

Figure 21 shows how the multi-objective optimization balances the profit against the operating cost savings for these values of the factor β . As expected, the cost savings decrease as we increase the importance of the profit collected by the energy storage owner. Going from $\beta = 0.001$ and

TABLE 4. EFFECT OF THE PROFIT MOTIVE ON THE OPTIMAL SITING DECISIONS

	β			
	0.001	0.01	0.1	1
1st	2374	4265	4259	4210
2nd	4259	4266	4265	4259
3rd	4337	4336	4337	4265
4th	4360	4337	4360	4267
5th	4361	4375	4375	4336
6th	4375	4376	4376	4337
7th	4376	4523	4382	4338
8th	4523	4528	4403	4375
9th	4528	4537	4523	4376
10th	4543	4543	4543	4523

$\beta = 0.01$ increases the profit of the storage owner by 64% at the expense of a 16% reduction in the cost savings that storage creates in the system. Increasing β from 0.1 to 1.0 leads to negative cost savings (i.e. a net increase in system cost!) but raises the profits by only 4%. Investments corresponding to the range from $\beta = 0.01$ to $\beta = 0.1$ are thus most likely to be both profitable for investors and valuable from an overall system perspective.

Figure 22 show how balancing cost and profit affects the total spillage of renewable energy and the total congestion surplus. The smallest amount renewable spillage is achieved for the lowest value of β . A moderate weight given to the profit motive minimizes the congestion surplus.

3.5 Effect of the number of storage locations

Figure 23 shows how the curve relating the total cost savings and the profit changes when we allow storage to be installed at 1, 5 or 10 locations. As expected, both the profit and the cost savings increase as we allow more storage installations. These curves suggest that allowing storage at more locations makes it possible to reduce costs while increasing profits. With fewer locations, these two objectives are more antagonistic.

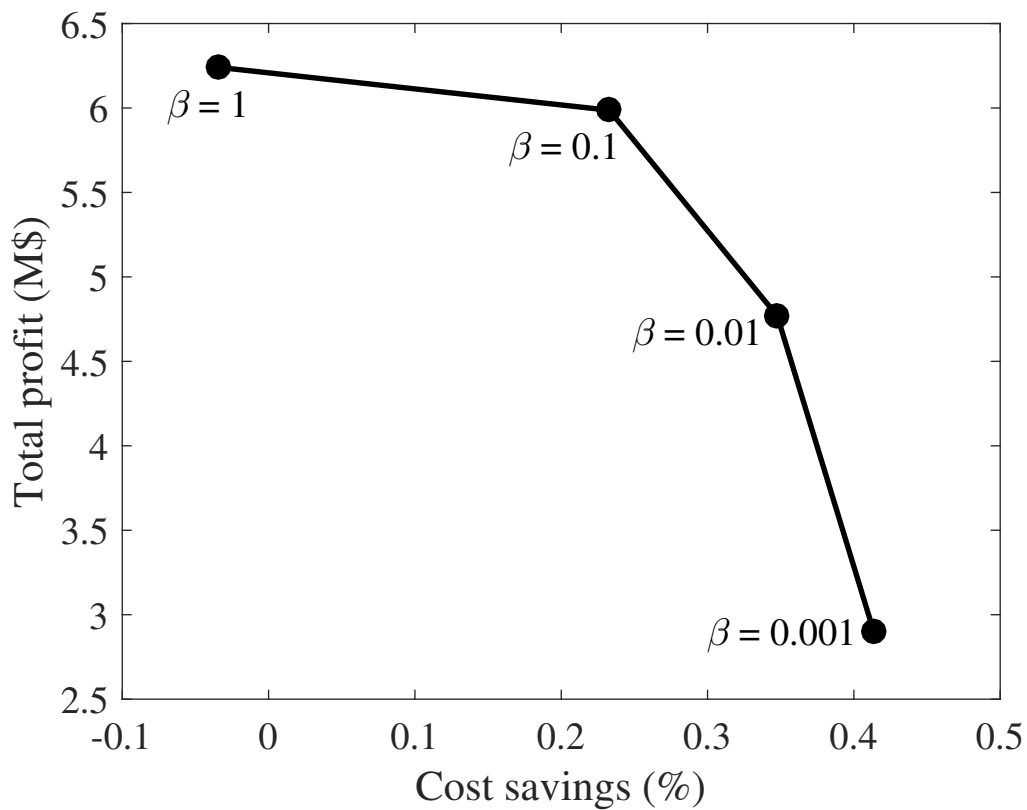


Fig. 21. Cost savings versus total profits

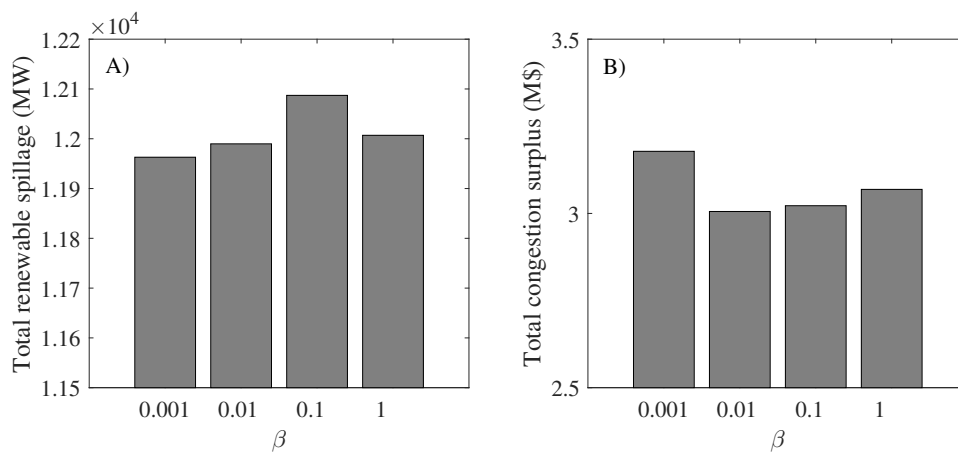


Fig. 22. Effect of balancing cost and profit on A) total renewable spillage and B) congestion surplus

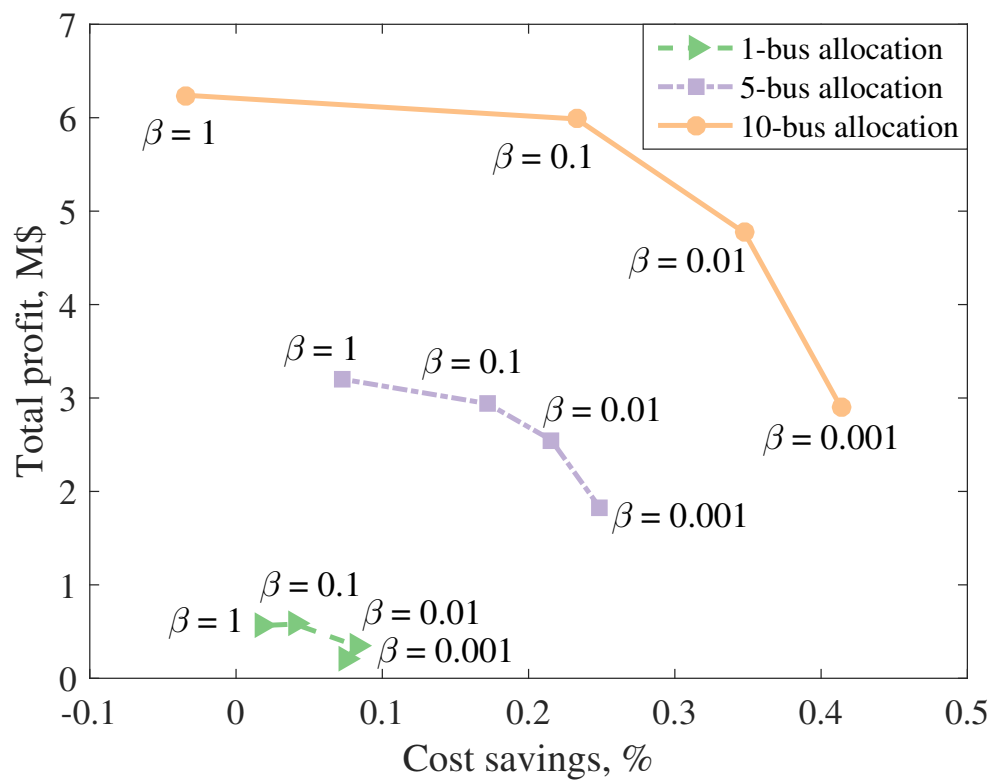


Fig. 23. Effect of the number of storage locations on the total cost savings and profit

4 Conclusions

This report considers the optimal siting and sizing of energy storage in large power systems from two different perspectives. First, those decisions are optimized from a centralized, cost minimization perspective. Then, a multi-objective optimization is used to examine how this cost minimization is related to the profit maximization that would be the goal of independent investors in energy storage. Both approaches are tested on realistic models of large power systems. The following observations can be made based on the result of the centralized, cost minimization formulation:

1. Reducing the penalty for spilling energy from renewable energy sources reduces the system operating cost but reduces the profit collected by the storage owners.
2. Storage tends to reduce renewable energy spillage, but this is not always the case.
3. Operating storage to minimize the total operating cost does not guarantee that investments in storage will be profitable. Including minimum profit constraints is therefore needed in models used for selecting investments in storage systems.
4. The proposed method is able to identify favorable storage locations on large systems.
5. These siting decisions are generally robust against the size of penalties for spilling renewable energy, the maximum allowed size of storage systems, and future projections of conventional units' marginal costs and increasing renewable production.

Considering both the cost savings resulting from the deployment of energy storage and the profitability of this storage leads to the following observations:

1. The siting decisions depend on the relative weight given to cost minimization and profit maximization.
2. The energy rating is limited by the artificial 50-MWh limit imposed on the size of energy storage systems. On the other hand the power rating increase when more weight is given to profit maximization.
3. Lower values of the weighting parameter β lead to a better trade-off between cost and profit.
4. Changing the relative weight of the cost and profit in the optimization does not significantly change the amount of renewable energy spilled or the congestion surplus.
5. Both the cost savings and the profits increase with the number of energy storage locations.

A Nomenclature

Sets and indices

\mathcal{B}	Set of buses, indexed by b .
$\hat{\mathcal{B}}$	Set of buses where ES can be installed, indexed by b .
\mathcal{E}	Set of representative days, indexed by e .
$\Omega^g(\Omega_b^g)$	Set of conventional or controllable generators (connected to bus b), indexed by i .
$\Omega^{rg}(\Omega_b^{rg})$	Set of renewable generators (connected to bus b), indexed by r .
$\Omega^{hp}(\Omega_b^{hp})$	Set of hydro generators (connected to bus b), indexed by h .
\mathcal{L}	Set of transmission lines, indexed by l .
\mathcal{O}_i	Set of segments of the cost curve of conventional generator i , indexed by o .
\mathcal{T}	Set of time intervals, indexed by t .
n	Auxiliary index of time intervals.
$o(l), d(l)$	Indices of origin and destination buses of line l .

Variables

All variables are per period t and representative day e unless otherwise indicated.

ch_{tbe}	Charging rate of the energy storage system connected to bus b .
c_b^{\max}	Maximum power rating of the energy storage system connected to bus b .
dis_{tbe}	Discharging rate of the energy storage system connected to bus b .
p_{tle}^f	Power flow on line l .
p_{tie}^g	Power output of conventional generator i .
p_{tioe}^g	Power output on segment o of the cost curve of generator i .
p_{the}^{hp}	Power output of hydro generator h .
s_{tbe}	State-of-charge of the energy storage system connected to bus b .
s_b^{\max}	Maximum energy rating of the storage system connected to bus b .
sp_{tre}^{rg}	Power spillage of renewable generator r .
v_{tie}	On/off status of conventional generator i .
y_{tie}	Start-up status of conventional generator i .
z_{tie}	Shutdown status of conventional generator i .
α_{tbe}	Binary variable representing whether an energy storage system is charging (1) or discharging (0).
β_{tbe}	Auxiliary continuous variable representing the nonlinear product $ch_{tbe}\alpha_{tbe}$.
θ_{tbe}	Voltage phase angle at bus b .
σ_b	Binary variable corresponding to the decision to locate an energy storage system at bus b .

Parameters

\bar{C}	Maximum power rating of an energy storage system.
C_{ioe}^E	Marginal cost of segment o of the cost curve of conventional generator i on representative day e .
C_i^{SU}	Start-up cost of conventional generator i .
C^S	Capital cost of an energy storage system per MWh.
C^P	Capital cost of an energy storage system per MW.
DT_i	Minimum down time of conventional generator i .
D_{tbe}	Demand at bus b during period t on representative day e .
N^{ES}	Number of energy storage locations.
N_{ie}^{DT}	Number of periods during which unit i must be initially scheduled off due to its minimum down time constraint on representative day e .
N_{ie}^{UT}	Number of periods during which unit i must be initially scheduled on due to its minimum up time constraint on representative day e .
\bar{P}_l^f	Maximum power flow on line l .
\bar{P}_{ioe}^g	Maximum power output on segment o of the cost curve of conventional generator i on representative day e .
\bar{P}_{ie}^g	Maximum power output of conventional generator i on representative day e .
\underline{P}_{ie}^g	Minimum power output of conventional generator i on representative day e .
\underline{P}_{the}^{hp}	Minimum power output of hydro plant h during time period t on representative day e .
\bar{P}_{the}^{hp}	Maximum power output of hydro plant h during time period t on representative day e .
P_{tre}^{rg}	Power output of renewable generator r during time period t on representative day e .
RD_i	Maximum ramp down rate of conventional generator i .
RU_i	Maximum ramp up rate of conventional generator i .
\bar{S}	Maximum energy rating of an energy storage system.
UT_i	Minimum up time of conventional generator i .
V_{ie}^0	Initial commitment of conventional generator i on representative day e .
$VoRS$	Value of renewable spillage.
x_l	Reactance of line l .
ρ	Energy-to-power ratio of an energy storage system.
$\eta^{c/d}$	Charging/discharging efficiency of energy storage system.
μ_e	Relative frequency of representative day e .

B Mathematical formulation of the cost minimization problem

The notation used in this formulation can be found in Appendix A. The objective function is:

$$\begin{aligned} \text{Minimize } & \sum_{e \in \mathcal{E}} \left[\mu_e \sum_{t \in \mathcal{T}} \sum_{i \in \Omega^g} \left(\sum_{o \in \mathcal{O}_i} C_{ioe}^E p_{tioe}^g + C_i^{SU} y_{tie} \right) \right] + \\ & \sum_{e \in \mathcal{E}} \left[\mu_e \sum_{t \in \mathcal{T}} \sum_{r \in \Omega^{rg}} \text{VORSS} p_{tre}^{rg} \right] + \sum_{b \in \mathcal{B}} \left(C^S s_b^{max} + C^P c_b^{max} \right), \end{aligned} \quad (1)$$

where the first term represents the expected operating cost over the representative days, including the dispatch and commitment costs of conventional generation; the second term is the expected value of the renewable energy spilled; and the last term denotes the daily pro-rated investment cost in energy storage, where parameters C^S and C^P are calculated based on the net present value approach [8].

The following subsections describe the constraints on this optimization problem.

Binary variables logic

The binary on/off status, start-up, and shutdown decisions are formulated as follows:

$$y_{tie} - z_{tie} = v_{tie} - v_{t-1,ie}; \forall t \in \mathcal{T}, \forall i \in \Omega^g, \forall e \in \mathcal{E} \quad (2)$$

$$y_{tie} + z_{tie} \leq 1; \forall t \in \mathcal{T}, \forall i \in \Omega^g, \forall e \in \mathcal{E}. \quad (3)$$

Constraint (2) determines whether unit i is started up or shut down at time t of representative day e based on the change in its on/off status between operating intervals t and $t-1$. Constraint (3) ensures that unit i cannot be started up and shut down during the same time interval of the representative day e .

Inter-temporal constraints

These constraints are modeled as:

$$v_{tie} = V_{ie}^0; \forall t \leq N_{ie}^{UT} + N_{ie}^{DT}, \forall i \in \Omega^g, \forall e \in \mathcal{E} \quad (4)$$

$$\sum_{n=t-UT_i+1}^t y_{rie} \leq v_{tie}; \forall t \in [N_{ie}^{UT}, n_T], \forall i \in \Omega^g, \forall e \in \mathcal{E} \quad (5)$$

$$\sum_{n=t-DT_i+1}^t z_{rie} \leq 1 - v_{tie}; \forall t \in [N_{ie}^{DT}, n_T], \forall i \in \Omega^g, \forall e \in \mathcal{E} \quad (6)$$

$$-RD_i \leq p_{tie}^g - p_{t-1,ie}^g \leq RU_i; \forall t \in \mathcal{T}, \forall i \in \Omega^g, \forall e \in \mathcal{E}. \quad (7)$$

Constraints (4)–(6) enforce the minimum up and down times. Constraint (7) models the ramp rate limits of the conventional units.

Generation dispatch constraints

The power outputs of conventional units, hydropower plants, and renewable generation units are constrained as follows:

$$p_{tie}^g = \sum_{o \in \mathcal{O}_i} p_{tioe}^g; \forall i \in \Omega^g, \forall t \in \mathcal{T}, \forall e \in \mathcal{E} \quad (8)$$

$$0 \leq p_{tioe}^g \leq \bar{P}_{ioe}^g; \forall o \in \mathcal{O}_i, \forall i \in \Omega^g, \forall t \in \mathcal{T}, \forall e \in \mathcal{E} \quad (9)$$

$$\underline{P}_{ie}^g \cdot v_{tie} \leq p_{tie}^g \leq \bar{P}_{ie}^g \cdot v_{tie}; \forall i \in \Omega^g, \forall t \in \mathcal{T}, \forall e \in \mathcal{E} \quad (10)$$

$$\underline{P}_{the}^{hp} \leq p_{the}^{hp} \leq \bar{P}_{the}^{hp}; \forall h \in \Omega^{hp}, \forall t \in \mathcal{T}, \forall e \in \mathcal{E} \quad (11)$$

$$0 \leq sp_{tre}^{rg} \leq P_{tre}^{rg}; \forall r \in \Omega^{rg}, \forall t \in \mathcal{T}, \forall e \in \mathcal{E} \quad (12)$$

Constraints (8)–(9) characterize the block structure of conventional generators. Constraints (10) enforce the minimum and maximum bounds on these units. Constraints (11) keep the hydropower production between its minimum and maximum limits. Finally, constraints (12) set the bounds for renewable generation spillage.

Network constraints

Network constraints are implemented using the following dc power flow model:

$$p_{tle}^f = \frac{1}{x_l} (\theta_{t,o(l),e} - \theta_{t,d(l),e}), \forall t \in \mathcal{T}, \forall l \in \mathcal{L}, \forall e \in \mathcal{E} \quad (13)$$

$$-\bar{P}_l^f \leq p_{tle}^f \leq \bar{P}_l^f, \forall t \in \mathcal{T}, \forall l \in \mathcal{L}, \forall e \in \mathcal{E}. \quad (14)$$

Constraint (13) computes the power flows on the network branches. Constraints (14) enforce the power flow limits.

Power balance constraint

The nodal power balance is formulated as follows:

$$\sum_{i \in \Omega_b^g} p_{tie}^g + \sum_{h \in \Omega_b^{hp}} p_{the}^{hp} + \sum_{r \in \Omega_b^{rg}} (P_{tre}^{rg} - sp_{tre}^{rg}) - \sum_{l|o(l)=b} p_{tle}^f + \sum_{l|d(l)=b} p_{tle}^f + dist_{tbe} = D_{tbe} + ch_{tbe},$$

$$\forall t \in \mathcal{T}, \forall b \in \mathcal{B}, \forall e \in \mathcal{E}. \quad (15)$$

Constraint (15) includes the injections of conventional and renewable generation, loads, adjacent transmission lines, as well as energy storage charging and discharging.

Constraints on energy storage systems

The constraints on energy storage systems are formulated as follows:

$$s_{tbe} = s_{t-1,be} + ch_{tbe}\eta^c - dis_{tbe}/\eta^d; \forall t \in \mathcal{T}, \forall b \in \mathcal{B}, \forall e \in \mathcal{E} \quad (16)$$

$$0 \leq s_{tbe} \leq s_b^{\max}; \forall t \in \mathcal{T}, \forall b \in \mathcal{B}, \forall e \in \mathcal{E} \quad (17)$$

$$0 \leq ch_{tbe}\eta^c \leq c_b^{\max}\alpha_{tbe}; \forall t \in \mathcal{T}, \forall b \in \mathcal{B}, \forall e \in \mathcal{E} \quad (18)$$

$$0 \leq dis_{tbe}/\eta^d \leq c_b^{\max}(1 - \alpha_{tbe}); \forall t \in \mathcal{T}, \forall b \in \mathcal{B}, \forall e \in \mathcal{E} \quad (19)$$

$$c_b^{\max}\rho \leq s_b^{\max}; \forall b \in \mathcal{B} \quad (20)$$

$$0 \leq s_b^{\max} \leq \bar{S}\sigma_b; \forall b \in \mathcal{B} \quad (21)$$

$$0 \leq c_b^{\max} \leq \bar{C}\sigma_b; \forall b \in \mathcal{B} \quad (22)$$

$$\sum_{b \in \hat{\mathcal{B}}} \sigma_b \leq N^{ES}. \quad (23)$$

Constraint (16) computes the ES state-of-charge. Constraints (17), (18)–(19) enforce respectively the energy and power ratings of ES. Constraints (18)–(19) preclude ES from simultaneously charging and discharging. Constraint (20) relates the energy and power ratings via an energy-power ratio determined by the chosen storage technology. Constraints (21)–(22) limit the maximum ES power and energy rating at each bus. Finally, constraint (23) allows placing only a number N^{ES} of energy storage system at a subset of buses $\hat{\mathcal{B}}$.

The optimization problem (1)–(23) is a nonlinear program because of the presence of products of continuous and binary decision variables ($c_b^{\max}\alpha_{tbe}$) in (18)–(19). These products can be linearized using integer algebra results [15]. Constraints (18)–(19) can be replaced with:

$$0 \leq ch_{tbe}\eta^c \leq \beta_{tbe}, \forall t \in \mathcal{T}, \forall b \in \mathcal{B}, \forall e \in \mathcal{E} \quad (24)$$

$$0 \leq dis_{tbe}/\eta^d \leq c_b^{\max} - \beta_{tbe}, \forall t \in \mathcal{T}, \forall b \in \mathcal{B}, \forall e \in \mathcal{E} \quad (25)$$

$$0 \leq \beta_{tbe} \leq \bar{C}\alpha_{tbe}, \forall t \in \mathcal{T}, \forall b \in \mathcal{B}, \forall e \in \mathcal{E} \quad (26)$$

$$0 \leq c_b^{\max} - \beta_{tbe} \leq \bar{C}(1 - \alpha_{tbe}), \forall t \in \mathcal{T}, \forall b \in \mathcal{B}, \forall e \in \mathcal{E}. \quad (27)$$

The stochastic ES siting and sizing problem to be solved for cost minimization is then the MILP problem given by (1)–(17), (20)–(27).

C Mathematical formulation of the multi-objective problem

For the sake of simplicity, let us assume that $C^{SO}(\cdot)$ represents the total expected operating cost, $C^{ES}(\cdot)$ is the investment cost in energy storage, and $P^{ES}(\cdot)$ is the total expected operating profit collected by energy storage. Then, the objective function of the multi-objective problem can be cast as follows:

$$\text{Minimize}_{\mathbf{u}, \mathbf{v}, \mathbf{w}} f(C^{SO}(\mathbf{u}, \mathbf{v}), C^{ES}(\mathbf{w}), P^{ES}(\hat{\lambda}, \mathbf{v}, \mathbf{w})) \quad (28)$$

subject to:

$$\mathbf{u} \in \Omega \quad (29)$$

$$h_1(\mathbf{u}, \mathbf{v}) \leq 0 \quad (30)$$

$$h_2(\mathbf{v}, \mathbf{w}) \leq 0 \quad (31)$$

$$h_3(\mathbf{v}) \leq 0, \quad (32)$$

where \mathbf{u} is the vector of binary variables, \mathbf{v} is the vector of continuous variables except for c_b^{max} and s_b^{max} , and $\mathbf{w} = \{c_b^{max}, s_b^{max}\}$. The total expected profits collected by energy storage can be written as:

$$P^{ES} = \sum_{e \in \mathcal{E}} \left[\mu_e \sum_{t \in \mathcal{T}} \sum_{b \in \mathcal{B}} \hat{\lambda}_{tbe} (dist_{tbe} - ch_{tbe}) \right]. \quad (33)$$

where the external parameter $\hat{\lambda}_{tbe}$ represents the locational marginal price paid by ES when charging and paid to ES when discharging. In this report, we assume that the locational marginal prices $\hat{\lambda}_{tbe}$ are equal to those from the unit commitment problem performed without energy storage.

As discussed in D, the CAISO system model based on the WECC 2024 planning model has uncontrollable resources or fixed generation, which include hydropower generation. In order to deal with numerical issues and unlike the problem formulation proposed in Appendix B, we penalize the spillage of hydropower generation (or fixed generation) in the objective function in a manner similar to renewable energy spillage.

Solution method

Several approaches have been proposed in the technical literature to address a multi-objective programming problem [4]. In order to combine the above-mentioned costs and profits into a single objective function, we use a method based on weighting factors which is hereinafter referred to as the β -based method. This method only weighs the second objective function and allows us to solve the multi-objective model with the same computational effort as the single-objective model [4]. It also allows us to compute different solutions by gradually increasing the value of parameter β , which ranges from 0 till 1. When $\beta = 0$, the multi-objective problem becomes a single-objective problem. In this case, it becomes a pure cost minimization. The objective function of problem (28)–(32) is expressed as:

$$f(C^{SO}(\mathbf{u}, \mathbf{v}), C^{ES}(\mathbf{w}), P^{ES}(\hat{\lambda}, \mathbf{v}, \mathbf{w})) = C^{SO}(\mathbf{u}, \mathbf{v}) + C^{ES}(\mathbf{w}) - \beta P^{ES}(\hat{\lambda}, \mathbf{v}, \mathbf{w}) \quad (34)$$

The formulation (34), (29)–(32) determines the optimal locations and sizes of ES for a given investment decision based on the total number of storage locations in a single shot. However, because of the large number of binary variables, this formulation is computationally expensive for large systems. In order to reduce this computational effort we can decompose the problem for each representative day. Then, instead of solving one stochastic problem, we first solve a separate problem for each representative day, considering that we can install ES at any location in the set

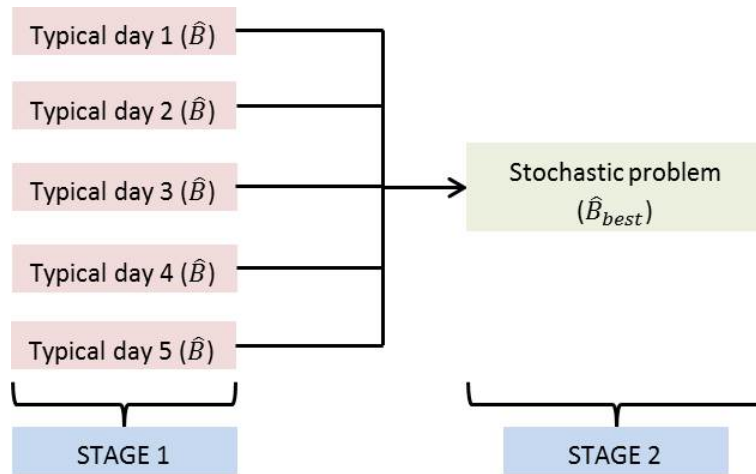


Fig. 24. Siting and sizing algorithm for large-scale systems.

of buses $\hat{\mathcal{B}}$). Then we solve the stochastic problem with a reduced set of buses where ES can be installed ($\hat{\mathcal{B}}_{best}$). Therefore, the siting and sizing algorithm is divided into two stages as shown in Fig. 24 and the computational effort for solving the stochastic problem is reduced.

D Handling of fixed generation

Our model of the CAISO system is based on the WECC 2024 planning model, which includes "uncontrollable resources" or "fixed generation". These include hydropower plants. Under some circumstances, this fixed generation must be adjusted to make the optimization problem feasible. To minimize these deviations, we penalize reductions in the output of these fixed generation sources in the objective function in the same way as renewable generation. The penalty for spillage can be either: (i) the same as the penalty for spilling renewable generation or (ii) Ten times greater than the highest *VoRS* that we consider (i.e. 1000 \$/MWh).

The following figures illustrate the effect of these penalties for the case without energy storage and for three different values of the *VoRS* (0, 50, and 100 \$/MWh). Figures 25 and 26 show the effect of these penalties on the generation costs, the fixed spillage costs, and the renewable costs for different values of *VoRS*. They show that the treatment of the fixed generation influences the generation and renewable spillage costs. How best to handle these fixed generators in the optimization would need to be discussed with the system operator.

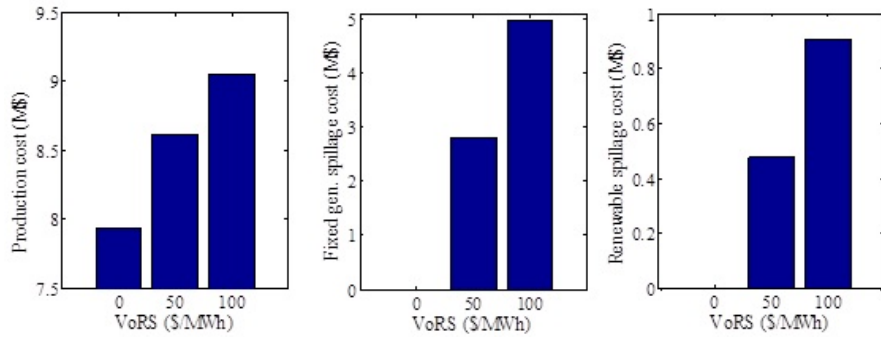


Fig. 25. Effect of the value of renewable energy spillage on the generation cost, the fixed generation spillage cost, and the renewable spillage cost when the penalty for fixed generation spillage is the same as the value of renewable energy spillage.

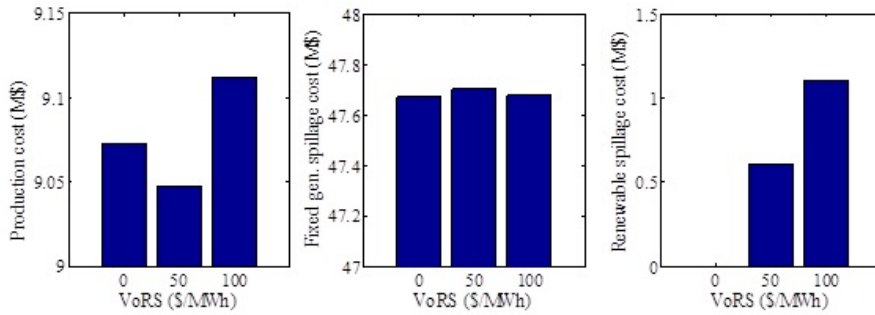


Fig. 26. Effect of the value of renewable energy spillage on the generation cost, the fixed generation spillage cost, and the renewable spillage cost when the penalty for fixed generation spillage is set at 1000 \$/MWh

References

- [1] J. Eyer and Garth Corey, “Energy storage for the electricity grid: Benefits and market potential assessment guide,” Technical report, Feb. 2010. [Online]. Available at: http://www.storagealliance.org/sites/default/files/whystorage/Sandia_Energy_Storage_Guide.pdf
- [2] A. Castillo and D. F. Gayme, “Grid-scale energy storage applications in renewable energy integration: A survey,” *Energy Conversion and Management*, vol. 87, pp. 885–894, Nov. 2014.
- [3] U.S. Department of Energy, “Grid energy storage,” Technical report, Dec. 2013. [Online]. Available at: http://www.sandia.gov/ess/docs/other/Grid_Energy_Storage_Dec_2013.pdf
- [4] M. Ehrgott, “A discussion of scalarization techniques for multiple objective integer programming,” *Ann. Oper. Res.*, no. 147, pp. 343–360, Aug, 2006.
- [5] L. Baringo and A. J. Conejo, “Strategic wind power investment,” *IEEE Trans. Power Syst.*, vol. 29, no. 3, pp. 1250–1260, May 2014.
- [6] J. E. Price and J. Goodin, “Reduced network modeling of WECC as a Market Design Prototype,” in *Proc. of the 2011 IEEE Power and Energy Society General Meeting*, 2011, pp. 1–5.
- [7] B. Pitt, “Applications of data mining techniques to electric load profiling”, *PhD thesis*, University of Manchester, UK, 2000. [Online]. Available at: http://www.ee.washington.edu/research/real/Library/Thesis/Barnaby_PITT.pdf
- [8] H. Pandžić, Y. Wang, T. Qiu, Y. Dvorkin, and D. S. Kirschen, “Near-optimal method for siting and sizing of distributed storage in a transmission network,” *IEEE Trans. Power Syst.*, vol. 30, no. 5, pp. 2288–2300, Sep. 2015.
- [9] B. Dunn, H. Kamath, and J.-M. Tarascon, “Electrical energy storage for the grid: A battery of choices,” *Science*, vol. 334, pp. 928–935, 2011.
- [10] “State renewable portfolio standards and goals,” 2016. [Online]. Available at: <http://www.ncsl.org/research/energy/renewable-portfolio-standards.aspx>
- [11] Hyak Supercomputer, 2016. [Online]. Available at: <http://goo.gl/X1ujJq>
- [12] The IBM ILOG CPLEX website, 2016. [Online]. Available: <http://www-01.ibm.com/software/commerce/optimization/cplex-optimizer>
- [13] R. E. Rosenthal, “GAMS – A Users Guide”, GAMS Corp., 2013.
- [14] The National Renewable Energy Laboratory, “Eastern wind integration and transmission study,” Technical report, Feb. 2011. [Online]. Available at: <http://www.nrel.gov/docs/fy11osti/47078.pdf>
- [15] C. A. Floudas, *Nonlinear and Mixed-Integer Optimization: Fundamentals and Applications*. New York, NY, USA: Oxford University Press, 1995.